Lack of Respiratory Chain Complex I Impairs Alternative Oxidase Engagement and Modulates Redox Signaling during Elicitor-Induced Cell Death in Tobacco

Guillaume Vidal,[a] Miquel Ribas-Carbo,[b] Marie Garmier,[a] Guy Dubertret,[a] Allan G. Rasmusson,[c] Chantal Mathieu,[a] Christine H. Foyer,[d] and Rosine De Paepe[a,1]

[a] Laboratoire Mitochondries et Métabolisme, Institut de Biotechnologie des Plantes, Unité Mixte de Recherche, Centre National de la Recherche Scientifique 8618, Université Paris Sud, 91 405 Orsay, France
[b] Grup de Recerca en Biologia de les Plantes en Condicions Mediterrànies, Departament de Biologia, Universitat de les Illes Balears, 07122 Palma de Mallorca, Spain
[c] Department of Cell and Organism Biology, Lund University, Sölvegatan 35B, SE-223 62 Lund, Sweden
[d] Crop Performance and Improvement Division, Rothamsted Research, Harpenden, Herts, AL5 2 JQ, United Kingdom

Alternative oxidase (AOX) functions in stress resistance by preventing accumulation of reactive oxygen species (ROS), but little is known about in vivo partitioning of electron flow between AOX and the cytochrome pathway. We investigated the relationships between AOX expression and in vivo activity in *Nicotiana sylvestris* and the complex I–deficient CMSII mutant in response to a cell death elicitor. While a specific *AOX1* isoform in the active reduced state was constitutively overexpressed in CMSII, partitioning through the alternative pathway was similar to the wild type. Lack of correlation between AOX content and activity indicates severe metabolic constraints in nonstressed mutant leaves. The bacterial elicitor harpin N_{Ea} induced similar timing and extent of cell death and a twofold respiratory burst in both genotypes with little change in AOX amounts. However, partitioning to AOX was increased twofold in the wild type but remained unchanged in CMSII. Oxidative phosphorylation modeling indicated a twofold ATP increase in both genotypes. By contrast, mitochondrial superoxide dismutase activity and reduced forms of ascorbate and glutathione were higher in CMSII than in the wild type. These results demonstrate genetically programmed flexibility of plant respiratory routes and antioxidants in response to elicitors and suggest that sustained ATP production, rather than AOX activity by itself or mitochondrial ROS, might be important for in planta cell death.

INTRODUCTION

Complexes I, III, and IV of the mitochondrial electron transport chain (ETC) operate in series to generate ATP. The mitochondria of plants and some fungi also possess non-proton-pumping respiratory enzymes that allow electron flow to occur in the absence of ATP generation. These include various alternative NAD(P)H dehydrogenases that bypass complex I (Rasmusson et al., 1999, 2004; Møller, 2001) and a cyanide-resistant terminal alternative oxidase (AOX) that branches from the main pathway at the level of the ubiquinone pool (Lambers, 1982; Vanlerberghe and McIntosh, 1997). The AOX therefore bypasses the energy conservation step performed by the proton-pumping cytochrome oxidase (COX) pathway.

The function of AOX activity was first characterized in thermogenesis in aroids (Meeuse, 1975). However, a large number of studies undertaken in the intervening period have revealed that AOX plays several important physiological roles (reviewed in Vanlerberghe and McIntosh, 1997). A key role of the AOX pathway is to prevent overreduction of the ETC and allow the continued operation of glycolysis and the tricarboxylic acid (TCA) cycle at times of high substrate availability, thus facilitating the oxidation of excess carbohydrate when ATP demand is low (Lambers, 1982). Accordingly, AOXs accumulate following pharmacological inhibition of the activities of complex III or IV (Vanlerberghe et al., 1994; Vanlerberghe and McIntosh, 1996, 1997; Sabar et al., 2000). Since overreduction of ETC components would inevitably increase the probability of formation of reactive oxygen species (ROS), AOX is considered to function in minimizing ROS generation (Wagner, 1995; Wagner and Krab, 1995; Purvis, 1997) and, hence, to decrease the likelihood of ensuing oxidative damage (Purvis and Shewfelt, 1993; Maxwell et al., 1999; Møller, 2001; Yip and Vanlerberghe, 2001). Enhanced AOX expression following exposure to biotic and abiotic stress conditions is consistent with this view. AOX transcripts are increased in response to pathogen attack (Lennon et al., 1997; Simons et al., 1999; Ordog et al., 2002), freezing and chilling (Vanlerberghe and McIntosh, 1992; Gonzalez-Meler et al., 1999), or low phosphate availability (Parsons et al., 1999; Juszczuk et al., 2001). However, much less information is available concerning the effects of stress on the in vivo activity of the enzyme and resultant changes in electron flow patterns. Currently, the in vivo activities of the AOX and COX pathways can only be

measured accurately by (^{18}O/^{16}O) oxygen isotope fractionation (Guy et al., 1989; Robinson et al., 1992, 1995; Ribas-Carbo et al., 1995, 1997, 2005a; Day et al., 1996). Such analyses have revealed increased in vivo AOX activity during abiotic stress responses, such as recovery from chilling stress (Ribas-Carbo et al., 2000), exposure to water deficits (Ribas-Carbo et al., 2005b), or herbicide treatment (Gaston et al., 2003). By contrast, there is little evidence of elevated AOX engagement during biotic stress responses in planta. For example, no significant changes in electron partitioning were observed in the incompatible reaction of *Nicotiana tabacum* leaves to tobacco mosaic virus (TMV), despite increased protein amounts (Lennon et al., 1997).

In this work, we investigated the relationships between AOX transcripts, protein, and in vivo activity in wild-type *Nicotiana sylvestris* and the mitochondrial CMSII mutant in response to a cell death elicitor. The mutant carries a deletion in its mitochondrial DNA (Li et al., 1988; Chétrit et al., 1992) encompassing the *nad7* gene encoding the highly conserved respiratory complex I NAD7 subunit (Pla et al., 1995; Lelandais et al., 1998). The absence of NAD7 results in a complete loss of complex I assembly and function (Gutierres et al., 1997; Sabar et al., 2000; Pineau et al., 2005). Constitutive enhancement of alternative NAD(P)H dehydrogenase activities compensates for the absence of complex I, resulting in an overall lower energetic efficiency of the mitochondrial ETC. Unexpectedly, CMSII plants possess high amounts of AOX transcripts and protein and increased capacity of cyanide-resistant respiration, as measured in isolated leaf mitochondria (Sabar et al., 2000). CMSII plants display an increased tolerance to ozone and enhanced resistance to an incompatible TMV interaction (Dutilleul et al., 2003b). Thus, a key question concerns whether the possession of constitutively high AOX protein content underpins the observed improved resistance of CMSII to abiotic and biotic stresses.

The first aim of this study was to determine whether AOX activity, measured under physiological conditions by oxygen isotope fractionation, is actually increased in CMSII compared with the wild type. The second aim was to examine the effects of an increased AOX capacity on the cell death responses induced by harpin N$_{Ea}$, a protein elicitor from *Erwinia amylovora* that leads to a hypersensitive-like response (HR) in nonhost plants such as tobacco and *Arabidopsis thaliana* (Wei et al., 1992).

RESULTS

Steady State Mitochondrial Electron Partitioning to AOX Is Not Increased in the CMSII Mutant

To determine whether the high protein amounts and AOX capacity in CMSII (Sabar et al., 2000) are associated with an increased in vivo AOX activity, we measured the partitioning of electrons through the AOX and COX pathways by (^{18}O/^{16}O) isotope fractionation. This technique is based on the fact that the two terminal oxidases fractionate (^{18}O/^{16}O) oxygen species differently, with the COX discriminating less than the AOX (Guy et al., 1989). Respiration, measured in the presence of either salicylhydroxamic acid (SHAM), an AOX inhibitor, or potassium cyanide (KCN), a complex IV inhibitor, gave discrimination values (Δ) of 21.3% ± 0.21% for COX and 30.1% ± 0.75% for AOX, respectively. These values are similar to those previously published for *N. tabacum* leaf discs (Lennon et al., 1997). The determined discrimination values were subsequently used to calculate electron partitioning between the COX and AOX pathways in the absence of inhibitors in wild-type and CMSII leaves. Uninhibited steady state respiration gave discrimination factors of 22.8% ± 0.2% for the wild type and 23% ± 0.5% for CMSII, corresponding to a partitioning through the alternative pathway (τa) of 0.20 in the wild type and 0.23 in CMSII (Table 1). Thus, despite the higher levels of AOX protein and catalytic capacity in CMSII, no changes in AOX partitioning were detected. The observed discrepancy between the high AOX capacity and true in vivo activity can be explained in at least three ways: (1) The abundant AOX protein forms of CMSII could be different to those found in the wild type. *AOX* homologs belong to a multigene family, comprising at least two subfamilies, termed *AOX1* and *AOX2*, which share limited nucleotide homologies (Saisho et al., 1997; Considine et al., 2002). *AOX* isogenes are tissue specific, show differential responses to respiratory inhibitors and environmental stresses, and could have different catalytic and regulatory properties. (2) The redox state of the AOX homodimer could be altered in CMSII. AOX is associated with the inner mitochondrial membrane as a homodimer (Andersson and Nordlund, 1999), with the two 35-kD polypeptides linked by a disulfide bridge in its oxidized form (Umbach and Siedow, 1993; Rhoads et al., 1998). The reduced form is more active than the covalently linked oxidized form in in vitro assays (Umbach and Siedow, 1993, 1996; Vanlerberghe et al., 1995; Ribas-Carbo et al., 1997). Therefore, it is conceivable that a larger pool of AOX protein that accumulates in the mutant is present in the less-active oxidized form. (3) There exists an increased metabolic control of AOX activity in the mutant, in relation with the observed changes in organic acid content (Dutilleul et al., 2005). Indeed, the enzyme is activated by pyruvate and other α-ketoacids in vitro (Millar et al., 1993; Day et al., 1994; Umbach et al., 1994; Vanlerberghe et al., 1999), although the activation state and the regulation of the enzyme in vivo have not been well characterized (Millenaar et al., 2001, 2002).

To examine the significance of each possible explanation with respect to the observed discrepancy between AOX protein

Table 1. Total Respiration Rate (Vt), Discrimination Factor (Δn), Activities of Cytochrome (v_{cyt}), and Alternative (v_{alt}) Pathways and Electron Partitioning through the Alternative Pathway (τa) in the Wild Type and CMSII

	Vt	Δn	v_{cyt}	v_{alt}	τa
Wild type	1.02 ± 0.18	22.82 ± 0.26	0.81 ± 0.14	0.20 ± 0.06	0.20 ± 0.03
CMSII	1.28 ± 0.06	23.0 ± 0.50	0.98 ± 0.03	0.30 ± 0.04	0.23 ± 0.02

The discrimination factors (Δn) are given in percentages, and respiratory activities are given in μmol O_2 m^{-2} s^{-1}. Values are means ± SD of at least three independent experiments. Calculations were made as described in Methods.

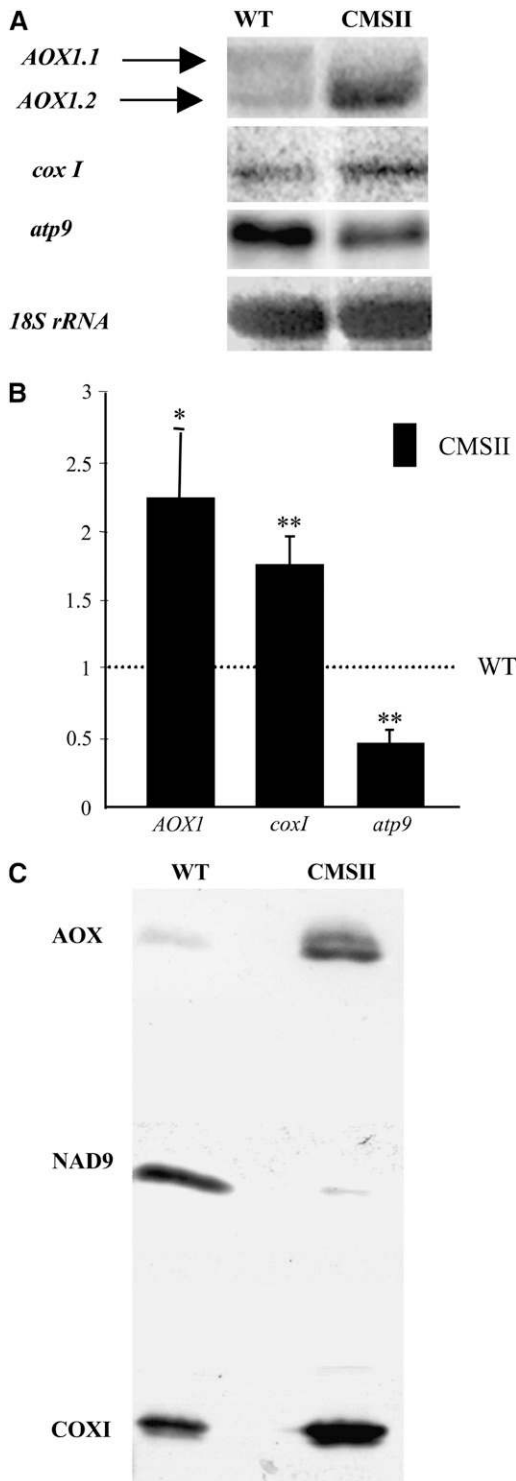content and activity, we have compared the abundance of transcripts, their response to respiratory inhibitors, and the relative redox state and regulation of the AOX protein in CMSII and wild-type plants as described below.

Accumulation of *AOX* Transcripts and Proteins

Using an *N. sylvestris AOX1* probe homologous to the *N. tabacum AOX1a* gene (Sabar et al., 2000) in long-run RNA gel blot experiments, we observed the accumulation of two types of AOX transcripts in mature leaves harvested in the middle of the illumination period (Figure 1A). These transcripts differed in length by <100 bp. For simplicity, we refer to the higher molecular weight band as *AOX1.1* and denote the smaller mRNA *AOX1.2*. The two *AOX1* transcripts were equally abundant in wild-type leaves, but the smaller mRNA dominated in CMSII (Figure 1A). When combined, the leaf *AOX1* transcript levels were twofold higher in CMSII relative to the wild type (Figure 1B). We also compared the accumulation of mitochondrial DNA-encoded transcripts between the genotypes. Steady state levels of *CoxI* transcripts encoding a catalytic subunit of complex IV were slightly increased, whereas those of *atp9* transcripts were lower in CMSII than in the wild type.

At the protein level, only one low-abundance AOX polypeptide could be detected by protein gel blotting in wild-type leaf mitochondria. On the other hand, two polypeptides were observed in CMSII extracts, the faster migrating band being the predominant species (Figure 1C). COXI protein was somewhat more abundant in the mutant, while the NAD9 complex I subunit was almost absent in CMSII compared with the wild type due to the mutation affecting complex I assembly (Gutierres et al., 1997).

To analyze whether the *AOX1.1* and *AOX1.2* transcripts were differentially regulated, we examined the responses to respiratory inhibitors (Figure 2). In addition to KCN and SHAM (described above), we used antimycin A (AA), an inhibitor of complex III. The plants showed symptoms in response to each inhibitor after a 24-h incubation, as determined by visual examination and

2000) and *atp9* and *coxI* mitochondrial sequences (Brangeon et al., 2000); *18S rDNA* was used as a loading control.

(B) Relative abundance of *AOX1* (pooled signals of *AOX1.1* and *AOX1.2*), *coxI*, and *atp9* transcripts in CMSII compared with the wild type (fixed to 1, dashed line). RNA gel blot signals were scanned with Scion imaging software and expressed as the values of the ratio: integrated density of the signal/integrated density of the *18S rRNA* signal. Values are the means ± SE from seven independent experiments. *AOX1* and *coxI* transcripts are more abundant, and *atp9* transcripts are less abundant in CMSII than in the wild type (*P < 0.05; **P < 0.01).

(C) Immunoblot of mitochondrial proteins from wild-type and CMSII leaves using a monoclonal *Sauromatum guttatum* anti-AOX antibody. Antibodies against NAD9, which is greatly decreased in CMSII leaves as a result of complex I assembly failure (Gutierres et al., 1997), and COXI were used as controls for loading and sample identity on the same membrane. Mitochondria were isolated from leaves as in Michalecka et al. (2004). Proteins (20 μg), as determined by the bicinchoninic acid method (Sigma-Aldrich), were loaded per lane by reducing SDS-PAGE on 10% acrylamide gels and wet electroblotted to nitrocellulose membranes in 10 mM CAPS, pH 11, and 20% methanol (v/v).
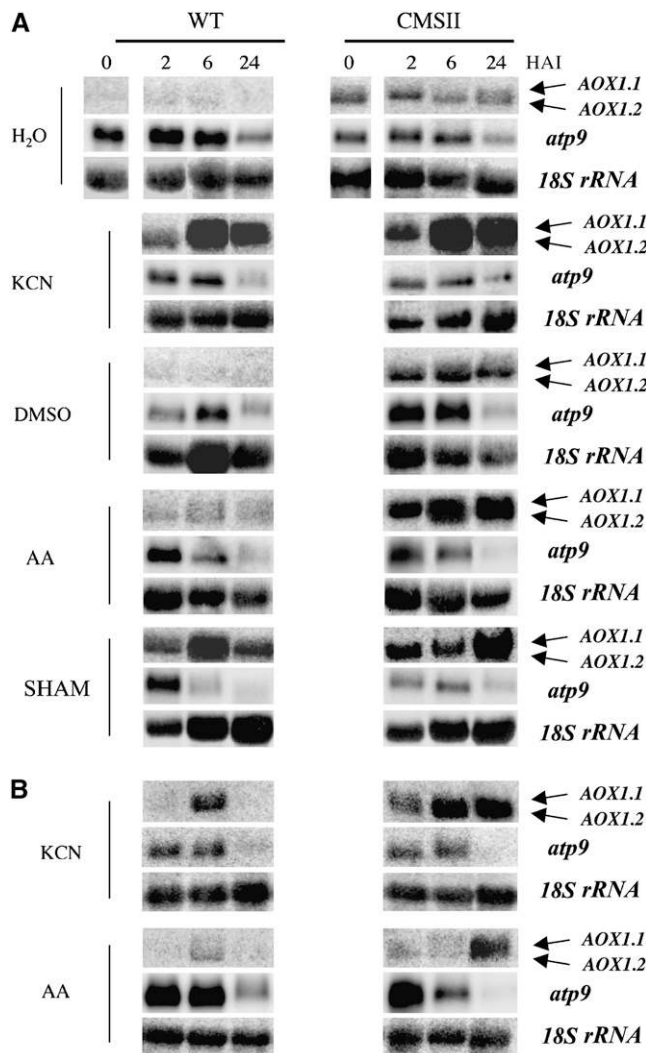
Figure 1. Comparative Analysis of AOX Expression in the Wild Type and CMSII Mutant.

(A) Total RNA was extracted from mature leaves of wild-type and CMSII plants and subjected to RNA gel blot analysis (12 μg RNA per lane) using as probes an *N. sylvestris AOX1* internal cDNA fragment (Sabar et al.,

Figure 2. RNA Gel Blot Analysis of *AOX* Gene Expression in Wild-Type and CMSII Plants Treated with Respiratory Inhibitors.

Plantlets were incubated in the complex IV inhibitor KCN (10 mM in water), the complex III inhibitor AA (100 μM dissolved in 1% DMSO), and the AOX inhibitor SHAM (10 mM in 1% DMSO). Water was used as control for KCN, and DMSO was used for the AA and SHAM treatments. RNA gel blot analysis was performed as described in Figure 1.

(A) Results of the full set of inhibitor treatments compared with water and DMSO controls. Experiments were repeated at least three times with similar results, and a typical experiment is shown.

(B) Less-exposed autoradiographs of RNA gel blots after KCN and AA treatments. These displays are from separate experiments compared with **(A)**.

by increased electrolyte leakage. At this time point, the wild-type plants were more affected than CMSII, and KCN had a stronger effect than the other inhibitors (Sabar et al., 2000; data not shown). KCN treatment strongly induced *AOX1* expression in both the wild type and CMSII, whereas AA and SHAM had less effect when compared with their respective controls (Figure 2A). In wild-type plants, *AOX1* hybridization signals peaked after a

6-h incubation with a given inhibitor, and *AOX1.2* transcripts accumulated more than *AOX1.1* transcripts, as clearly seen in the less-exposed autoradiographs (Figure 2B). In CMSII, *AOX1* induction continued over a longer time period when compared with the wild type (Figures 2A and 2B). In contrast with the nuclear-encoded *AOX1* transcripts, levels of mitochondrial *atp9* transcripts were unaffected by the different inhibitor treatments but decreased in both genotypes over the 24-h period, also after incubation with water or DMSO alone.

Taken together, these results showed that the *AOX1.2* gene is overexpressed in CMSII. The expression of *AOX1.2* is more responsive than *AOX1.1* to respiratory inhibitors.

Redox State of AOX Homodimers in Whole Leaves and Isolated Mitochondria

We examined whether the low in vivo AOX activity in CMSII could be due to an altered redox state of the enzyme. For this, we used nonreducing SDS-PAGE electrophoresis followed by protein gel blotting. In wild-type leaf extracts, only the 35-kD monomeric form could be detected (Figure 3A), consistent with previous reports on other leaf tissues, including tobacco (Umbach and
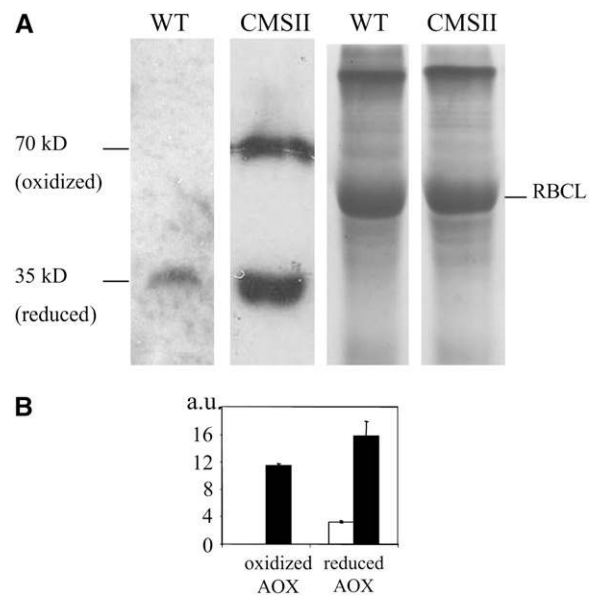

Figure 3. Redox State of Leaf AOX Proteins.

Total leaf protein from wild-type and CMSII leaves was extracted as described in Methods and separated by nonreducing SDS-PAGE on 12% acrylamide gels (40 μg per lane). After electrotransfer to nitrocellulose membranes, proteins were probed with *S. guttatum* anti-AOX antibody and detected by chemiluminescence.

(A) Left: immunoblot; reduced (35 kD) and oxidized (70 kD) forms of the AOX homodimer are indicated. Right: Coomassie blue–stained gel showing control loading; the 55-kD ribulose-1,5-bisphosphate carboxylase/oxygenase (Rubisco) large subunit (RBCL) is indicated.

(B) Quantification of the reduced and oxidized AOX forms in wild-type and CMSII leaves (arbitrary units [a.u.]). Protein gel blot signals were scanned with Scion imaging software. Wild type, open bar; CMSII, closed bars. Values are the means ± SE from three independent experiments

Siedow, 1997; Vanlerberghe et al., 1999). On the contrary, CMSII was found to contain significant amounts of the covalently linked, oxidized, 70-kD homodimer (Figure 3A), representing ~40% of the total AOX protein content (Figure 3B). Still, there is substantially more reduced AOX protein in CMSII than in the wild type.

We then examined the effect of organic acids on AOX redox state in Percoll-purified leaf mitochondria. The AOX proteins extracted from wild-type mitochondria essentially migrated as 70-kD dimers in nonreducing gels (Figure 4). Such oxidation of AOX proteins during mitochondrial isolation has previously been
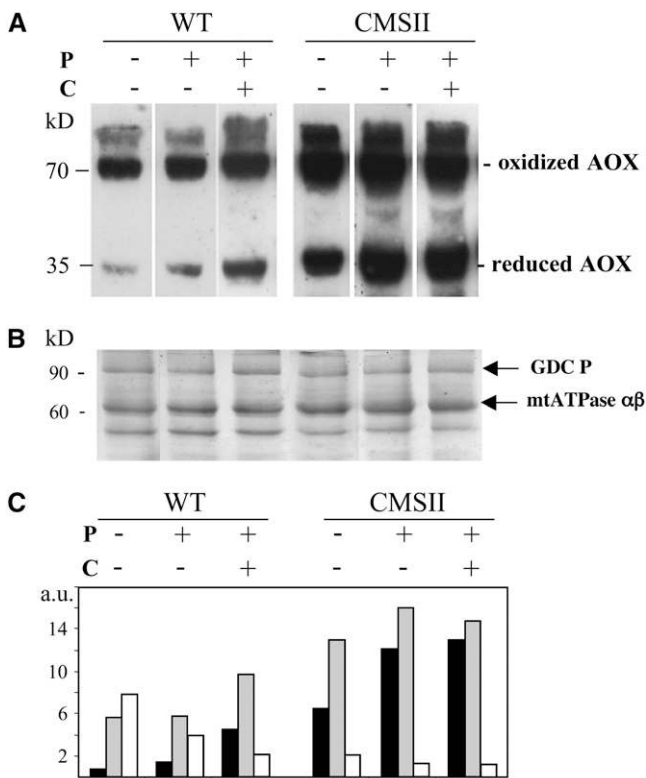

Figure 4. Effects of Pyruvate and Citrate on the AOX Redox State of Purified Leaf Mitochondria.

Mitochondria from *N. sylvestris* wild-type and CMSII leaves were isolated as described in Methods. Pyruvate (P) at 5 mM was added (+) or not (−) to all buffers during the mitochondrial isolation process. Purified mitochondria were resuspended in the washing buffer, supplemented (+) or not (−) with 20 mM citrate (C), incubated for 1 h, and then pelleted by centrifugation.

(A) Immunodetection of reduced and oxidized forms of AOX. Mitochondrial proteins (50 μg per lane) were separated by nonreducing SDS-PAGE on 12% acrylamide gels. After electrotransfer to nitrocellulose membranes, proteins were probed with *S. guttatum* anti-AOX antibody and detected by chemiluminescence.

(B) Coomassie blue–stained control gel of mitochondrial proteins. The quality of the mitochondrial preparations is demonstrated by the presence of the P subunit of glycine decarboxylase (GDC P) and the αβ-subunits of mitochondrial ATPase (~60 kD; De Paepe et al., 1993).

(C) Quantification of oxidized and reduced forms of AOX. Reduced AOX, black bars; oxidized AOX, gray bars; ratios of oxidized/reduced forms of AOX, white bars.

reported in *N. tabacum* and other plant species (Vanlerberghe et al., 1999). In marked contrast, a significant proportion (30%) of AOX proteins was still in the reduced state in CMSII mitochondria. The presence of 5 mM pyruvate in the mitochondrial isolation media partially prevented AOX oxidation in both genotypes, with the proportion of AOX monomers being ~40% in CMSII and below 20% in the wild type (Figure 4C). Incubation of isolated mitochondria with citrate allowed a further reduction of the protein in the wild type but not in the mutant. These results suggest a lower propensity of the redox active thiol groups to become oxidized during CMSII mitochondrial preparations. This could be caused by the higher total endogenous organic acid pools in the mutant (Dutilleul et al., 2005). Alternatively, the redox properties of the two AOX isoforms described above (Figure 1) may be different.

These results show that the relatively low in vivo AOX activity in CMSII cannot be explained by extensive oxidation of the homodimer. However, studies on isolated mitochondria indicated that the dynamic adjustment of the AOX redox state might be altered in the mutant.

Effects of in Planta Elicitation by Harpin N_{Ea} on AOX Activity and Expression

We investigated whether the constitutively high AOX capacity of CMSII leaves was exploited during the HR-like response induced by the bacterial elicitor harpin N_{Ea}. First symptoms (i.e., glittering of the infiltrated zone) developed 4 to 6 h after harpin inoculation (HAI) in both genotypes (Figure 5A). Tissue damage was apparent by 24 HAI, and necrosis was complete at 48 HAI. The time course of cell death was estimated by electrolyte leakage, a technique commonly used as an in planta cell death marker (Pike et al., 1998). The kinetics of electrolyte leakage after harpin infiltration were similar in both genotypes (Figure 5B). Electrolyte loss reached a plateau at 24 HAI, suggesting that most cells had lost plasma membrane integrity at this time point. Infiltration with buffer did not induce necrotic symptoms or electrolyte leakage.

No significant changes in respiration were observed following buffer infiltration, but harpin induced a marked increase in total oxygen consumption (V_{tot}) for several hours in both genotypes (Figure 6). Respiration rates peaked 8 HAI at 2.7 μmol $O_2 \cdot m^{-2} s^{-1}$ in CMSII and at 2.4 μmol $O_2 \cdot m^{-2} s^{-1}$ in the wild type. The rates were similar to control levels at 24 HAI and were close to zero at 48 h pi, in good agreement with a complete cell death at this time point. In contrast with global respiratory changes, electron partitioning between the COX and the AOX pathways was differently affected by the elicitor in wild-type and CMSII leaves. In the wild type, the participation of AOX (τa) increased from 0.20 in control leaves to 0.38 at 4 HAI and to 0.43 at 8 HAI (Table 2). At this time point, almost 50% of the electrons flowing through the respiratory chain were engaged in fluxes through the AOX pathway. By 24 HAI, τa was below the control value of 0.12. In absolute terms, the alternative pathway activity (v_{alt}) increased transiently over the first 8 HAI from 0.20 to 1.03 μmol $O_2 \cdot m^{-2} s^{-1}$ (Figure 7A, open symbols). By contrast, the COX pathway (v_{cyt}) showed only a small harpin-induced increase, from 0.81 to 1.35 μmol $O_2 \cdot m^{-2} s^{-1}$ in the same time period (Figure 7B, open symbols). In CMSII, the participation of AOX did not significantly
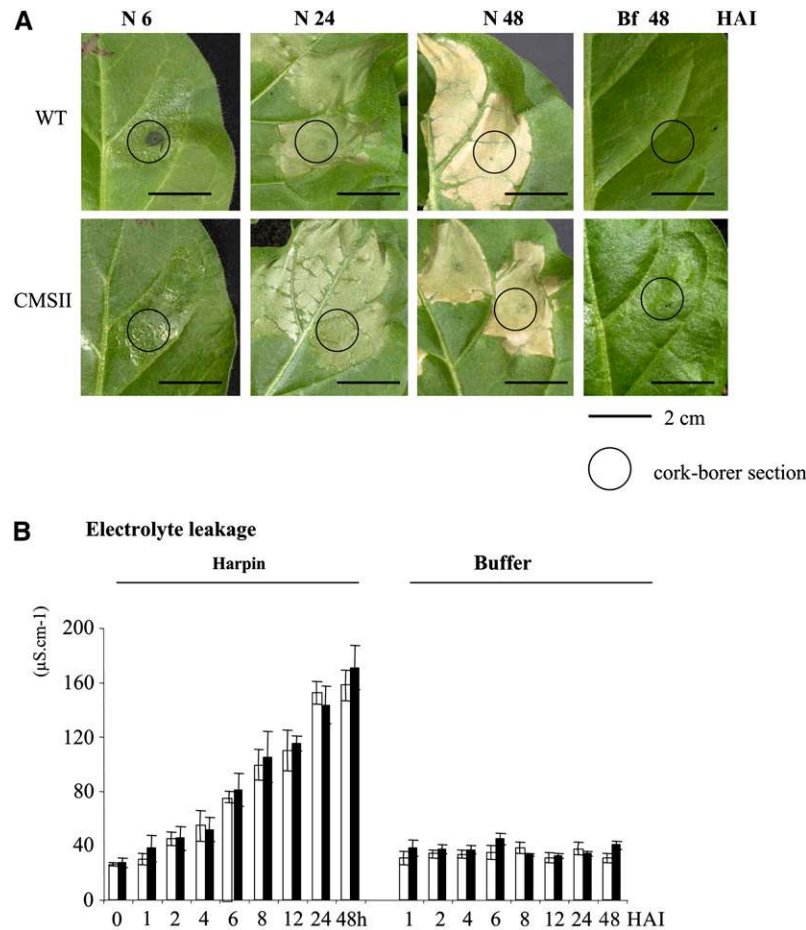
Figure 5. Cell Death–Associated Symptoms Induced by Harpin.

(A) Progression of necrotic symptoms in wild-type and CMSII leaves. Harpin at 40 μg·mL^{-1} was inoculated with a syringe on the abaxial face of the second well-developed leaf. At different times after harpin (N 6, N 24, and N 48) or buffer (Bf 48) infiltration, discs were punched out with a cork-borer from the central area of treated tissues, as indicated by circles.

(B) Electrolyte leakage measurements. Samples were harvested at different times (in hours) after harpin or buffer infiltrations into wild-type (open bars) or CMSII (closed bars) foliar tissues and placed in distilled water, and measurements were performed as described in Methods. Extracellular conductivity is expressed as μS cm^{-1}. Values are means $\pm$ SE from at least three independent experiments.

change after harpin elicitation (Table 2). Oxygen consumption by the two respiratory pathways instead increased in parallel during the first 8 HAI in response to harpin, reaching twofold increases over the preinoculation values. Thus, v_{alt} progressively increased from 0.30 to 0.62 μmol O$_2$·m^{-2}s^{-1} at 8 HAI (Figure 7A, closed symbols) and v_{cyt} from 0.98 to 2.07 μmol O$_2$·m^{-2}s^{-1} at 8 HAI (Figure 7B, closed symbols). However, by 24 HAI, fluxes through both pathways were similar or lower than the control values. No partitioning changes were observed after buffer treatments in either genotype (data not shown).

Since CMSII is deficient in complex I, the first site of proton pumping of the respiratory chain, these data allow a unique possibility for modeling ATP production in plants with different stoichiometries of ATP production per oxygen consumed. Such an analysis revealed that a virtually identical increase in ATP production took place in wild-type and CMSII plants throughout the period of post-harpin respiratory enhancement, except when the cells approached necrosis at 24 HAI (Figure 7C). The wild-type and CMSII values for 0 to 24 HAI were positively correlated ($P < 0.01$; $r = 0.96$) in the two-tailed Pearson analysis. In this model, we assumed that respiration in dark-adapted leaves used glucose (or sucrose) via standard glycolysis and TCA cycle pathways (Table 3). Modeling based on malate consumption lowered ATP production at each time point by ~3 and 11.5% for the wild type and CMSII, respectively. Similarly, if sucrose is metabolized via PPi-linked glycolytic enzymes, ATP production at each point would increase by ~8.5 and 11% for the wild type and CMSII, respectively (data not shown). Thus, irrespective of substrate used for the model, the results show that the plants modulate electron partitioning between the COX and AOX pathways to adapt ATP production to the cellular demand during cell death.
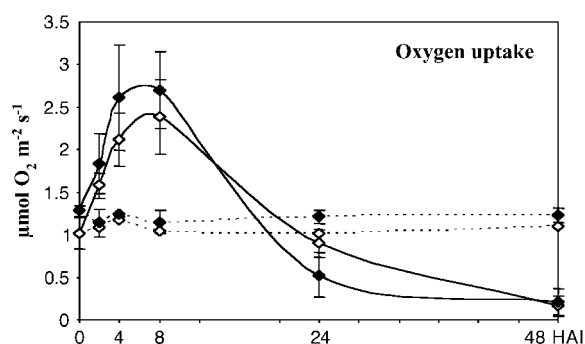
Figure 6. Total Respiration Rates (V_{tot}) in Harpin-Elicited Leaves.

Leaf disks were harvested at different times (in hours) after harpin (40 $\mu g \cdot mL^{-1}$) or buffer infiltration into wild-type or CMSII foliar tissues. Wild type, open symbols; CMSII, closed symbols; dashed lines, buffer. Values are means ± SD from at least three independent experiments.

We examined whether the induction of AOX activity following harpin infiltration was related to expression changes. In the wild type, we observed an almost threefold increase in *AOX1* transcripts accumulation at 1 HAI compared with the control (Figure 8). This change specifically involved the *AOX1.2* transcript and was only transient, since transcripts dropped down to the basal level at 3 HAI. By contrast, no transcript changes were observed in CMSII. In both genotypes, steady state levels of *coxI* transcripts remained unchanged after elicitation.

Using protein gel blotting of nonreduced gels, no clear-cut effect of harpin was observed until after 12 HAI in any of the genotypes regarding AOX content and redox state (Figure 9). At 12 HAI, a limited increase in AOX protein was observed in both genotypes. However, at 24 HAI, approximately half of the AOX proteins had become present in the oxidized state, and this could partially explain the loss of AOX activity observed at this time point (Figure 7). Buffer treatment affected neither abundance nor redox state of the AOX protein in either genotype.

Transcript and protein studies clearly show that the rapid harpin-induced AOX activity changes observed from 4 HAI (Figure 7) are essentially controlled at the posttranslational level.

Differential Effects of Harpin on Mitochondrial and Extramitochondrial Antioxidants

The harpin-induced respiratory burst might give rise to an increased respiratory generation of ROS that could act as a secondary messenger triggering the HR-like process. Superoxide generated by the mitochondrial ETC at the level of complexes I and III (Møller, 2001) is converted to hydrogen peroxide by either

spontaneous dismutation or much more efficiently by mitochondrial superoxide dismutase (MnSOD). As mitochondrial ROS are difficult to measure in planta, we examined SOD activities in harpin-elicited wild-type and CMSII leaves using an in-gel procedure. In nonelicited leaves, MnSOD activity was significantly higher ($P < 0.05$) in CMSII compared with the wild type. After elicitation, MnSOD activity decreased slowly in both genotypes, with the pooled 8- to 24-h values being significantly lower than the pooled 0- to 2-h values ($P < 0.05$). These results indicate that higher amounts of hydrogen peroxide are generated by CMSII mitochondria compared with wild-type mitochondria during elicitation, in good agreement with the increased COX activity. By contrast, chloroplastic FeSOD activities were similar in wild-type and CMSII leaves and did not markedly change until 24 HAI. Neither MnSOD nor FeSOD activities were affected by buffer treatments (data not shown).

In addition to ROS, soluble antioxidants have been shown to be important players in the control of oxidative stress (Noctor and Foyer, 1998). We compared content and redox state of ascorbate and gluthatione, the major soluble antioxidants of plant cells, during harpin-induced HR. Interestingly, the last enzyme in the ascorbate biosynthetic pathway is mitochondrial L-galactono-1, 4-lactone dehydrogenase, the activity of which is linked to electron fluxes between complexes III and IV (Millar et al., 2003). Untreated wild-type and CMSII leaves contained similar amounts of ascorbate (Figure 11). However, while the ascorbate content of the wild-type leaves progressively decreased after harpin inoculation, the CMSII leaves retained their initial ascorbate pool size until 14 HAI (Figure 11). At the 36-h time point, wild-type and CMSII leaves contained 15 and 60% of their initial ascorbate content, respectively. On the other hand, the total glutathione content was higher in CMSII leaves compared with the wild type. In both genotypes, the total glutathione pool increased transiently following the harpin treatment. The redox state of the harpin-elicited leaves became markedly affected after 24 HAI, as indicated by an increased oxidation level of both the ascorbate and glutathione pools (Figure 11). For both soluble antioxidants, the elicitor-induced changes in oxidation state were delayed in CMSII compared with wild-type leaves.

DISCUSSION

Lack of Correlation between AOX Protein Content and in Vivo Activity

Despite the dramatic increase in the AOX protein content of CMSII leaves compared with the wild type (Gutierres et al., 1997; Sabar et al., 2000; Dutilleul et al., 2003a, 2003b; this work), the partitioning of electrons to the AOX pathway was close to 0.2 in

Table 2. Partitioning through the Alternative Pathway (τa) in Wild-Type and CMSII Leaves during Harpin-Induced Cell Death

	0	2 h	4 h	8 h	24 HAI
Wild type	0.20 ± 0.03	0.24 ± 0.05	0.38 ± 0.05	0.43 ± 0.03	0.12 ± 0.01
CMSII	0.23 ± 0.02	0.27 ± 0.04	0.24 ± 0.02	0.23 ± 0.03	0.27 ± 0.05

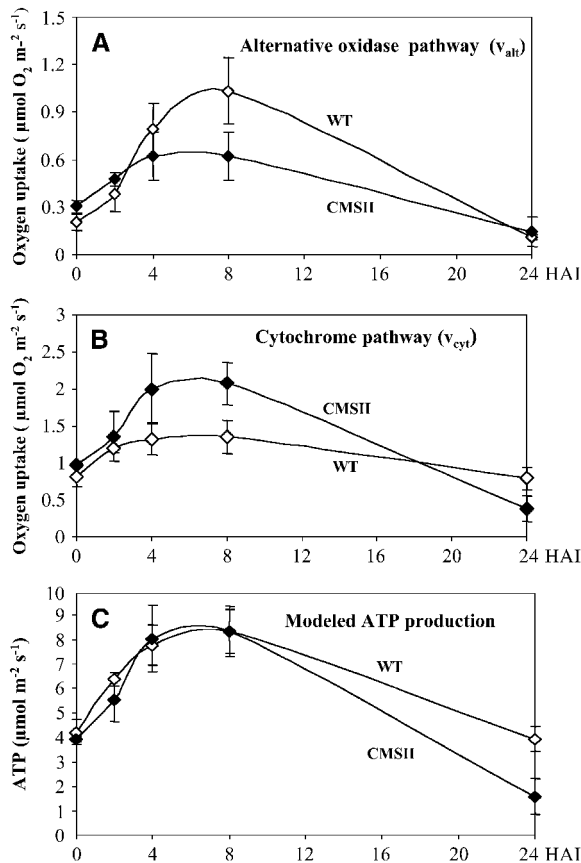Values are means ± SD of at least three independent experiments.

Figure 7. Changes in the Cytochrome (v_{cyt}) and Alternative (v_{alt}) Pathway Activities in Harpin-Elicited Leaves.

Leaf disks were harvested at different times (in hours) after harpin (40 $\mu g \cdot mL^{-1}$) or buffer infiltration into wild-type or CMSII foliar tissues. Wild type, open symbols; CMSII, closed symbols. Values are means ± SD from three independent experiments. Calculations were made as described in Methods.
(A) Activity of the AOX pathway.
(B) Activity of the cytochrome pathway (COX).
(C) Modeling of ATP production for dark respiration driven by glucose catabolism (see Table 3).

are overexpressed by inhibitor treatments in different NCS mitochondrial mutants, including the NCS2 complex I mutant (Karpova et al., 2002). KCN treatment has been shown to induce hydrogen peroxide accumulation (Umbach et al., 2006). Thus, the *AOX1.2* gene may be constitutively overexpressed in CMSII due to superoxide and/or hydrogen peroxide overproduction by the respiratory chain, in good agreement with the observed higher MnSOD activity (Figure 10). Moreover, *AOX1* transcript accumulation was differentially regulated in CMSII compared with the wild type. *AOX1* induction continued over a longer time period during inhibitor treatments (Figure 2B). By contrast, *AOX1* transcripts did not accumulate in CMSII leaves after harpin treatment as they did in the wild type. These results indicate altered signaling of *AOX1* expression in CMSII. By contrast, the regulation of mitochondrial respiratory gene expression (*coxI* and *atp9*) was similar in wild-type and mutant leaves.

Furthermore, two polypeptides reacting with the anti-AOX antibodies were observed in CMSII, the lower molecular weight polypeptide being more abundant than in the wild type (Figure 1C). This shows that at least two different AOX isoforms are present in CMSII mitochondria, possibly corresponding to the two *AOX1* transcripts described above. Unfortunately, it is not known whether these two AOX forms exhibit different specific activities. To the best of our knowledge, clear differences in the activity of AOX isoforms have not been reported in any species. On the other hand, small changes in amino acid sequence can mediate differences in specificity for the allosteric activator (Umbach et al., 2006). Thus, while the balance between two differentially expressed AOX isoforms might be important for

Table 3. Modeling ATP Production in Wild-Type and CMSII Plants

Glc-O$_2$		ATP/Glc			
		WT-COX	WT-AOX	CMS-COX	CMS-AOX
Glycolysis	2 ATP/Glc	2	2	2	2
	2 NADH/Glc	3	1	3	1
TCA cycle	2 ATP/Glc	2	2	2	2
	2 FADH$_2$/Glc	3	0	3	0
	8 NADH/Glc	18.4	6.4	12	2
Total		28.4	11.4	22	7

Malate-O$_2$		ATP/Malate			
		WT-COX	WT-AOX	CMS-COX	CMS-AOX
Malic enzyme	1 NADH/mal	2.3	0.8	1.5	0.25
TCA cycle	1 ATP/mal	1	1	1	1
	4 NADH/mal	9.2	3.2	6	1
	1 FADH$_2$/mal	1.5	0	1.5	0
Total		14	5	10	2.25

In the top part of the table, ATP/O$_2$ for in vivo respiration was calculated for complete catabolism of glucose (Glc) via AOX and COX pathways separately in wild-type and CMSII plants. Sucrose degradation via invertase gives the same result. Sucrose degradation via PPi-using glycolytic enzymes increases the direct yield of ATP from glycolysis to four per Glc (Browse et al., 2006). The ATP/Glc corresponds to 6 times ATP/O$_2$. In the bottom part of the table, the same calculation is shown for malate, with ATP/malate corresponding to 3 times ATP/O$_2$. Stoichiometries used are described in Methods.

both genotypes. Such an absence of correlation between AOX expression and activity in CMSII could be explained by the expression of a different isoform with a lower activity, a modified redox state, or an altered biochemical regulation.

Our results suggest that the major AOX isoform expressed in CMSII mature leaves might be different from the dominant isoform in wild-type leaves. The higher *AOX1* transcript levels in CMSII leaves were essentially due to the specific accumulation of the lower molecular weight *AOX1.2* mRNA. In the wild type, *AOX1.2* was more responsive than *AOX1.1* to treatment with respiratory inhibitors (Figure 2) and harpin (Figure 8). In *Arabidopsis* and soybean (*Glycine max*), the *AOX1* family comprises several tissue-specific isogenes that respond differentially to respiratory inhibitors (Saisho et al., 1997; Considine et al., 2002; Clifton et al., 2006). In maize (*Zea mays*), specific *AOX* transcripts
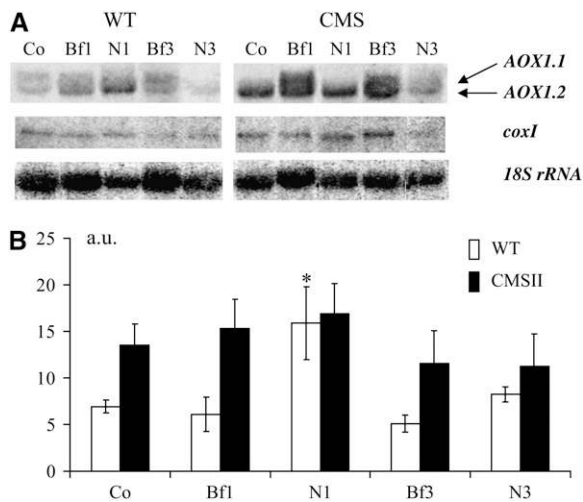
Figure 8. Transient Changes in *AOX1* Transcript Accumulation after Harpin Elicitation.

Harpin or buffer was inoculated as indicated in Figure 5. Samples were harvested at the times indicated after the treatments; total RNA was isolated and run on a 1.3% agarose gel (12 μg per lane). Co, control before elicitation; N, harpin; Bf, buffer.

(A) RNA gel blot analyses using an *N. sylvestris AOX1* internal cDNA fragment and *coxI* sequence as probes; *18S rDNA* was used as a loading control. Experiments were repeated three times with similar results, and a typical experiment is shown.

(B) Relative abundance of pooled *AOX1.1* and *AOX1.2* signals in the wild type and CMSII. RNA gel blot signals were scanned with Scion imaging software. Results are expressed as ratios between *AOX1* signal density and *18S rRNA* signal density. Wild type, open bars; CMSII, closed bars. In the wild type, the increase in the pooled *AOX1* transcripts 1 HAI (N1) compared with the control (Co) is significant (*$P < 0.05$). Values are the means ± SE from seven independent experiments.

modulating in vivo activity, biochemical or physiological regulations have to be taken into account. Although the low-activity oxidized AOX homodimer can be detected immunologically in CMSII leaf extracts, the reduced form predominates in both CMSII and wild-type leaves. This indicates that the low electron partitioning through the AOX pathway in CMSII leaves is not due to extensive oxidation of the enzyme. Moreover, the AOX homodimer is less subjected to oxidation during mitochondrial isolation in CMSII than in the wild type and is less responsive to organic acids in vitro. This may be due to differences in the redox reactivity between the two AOX isoforms. Alternatively, the in vivo change in AOX oxidation status in CMSII could derive from the perturbation of matrix redox chemistry resulting from the deficiency in complex I that was previously reported (Dutilleul et al., 2003b). Regulation of AOX activity by mitochondrial metabolites is of key importance. In vitro, a positive correlation between AOX expression and capacity and the amounts of certain TCA cycle substrates, particularly citrate, isocitrate, and malate, has been demonstrated in tobacco mitochondria (Lennon et al., 1995; Vanlerberghe et al., 1995; Millar et al., 1996; Vanlerberghe and McIntosh, 1996). However, citrate added to detached *Poa annua* roots induced AOX protein but abolished in vivo activity

(Millenaar et al., 2002). CMSII leaves contain twice as much citrate as wild-type leaves under the same conditions (Dutilleul et al., 2005), and this may explain both the AOX overexpression and the lack of in vivo activity. In addition, CMSII leaves have less than half the amount of 2-oxoglutarate measured in wild-type leaves (Dutilleul et al., 2005). Since 2-oxoglutarate has also been found to positively regulate AOX activity (Vanlerberghe et al., 1995), the depletion of this metabolite may further decrease AOX activity in the CMSII plants.

Collectively, these data support the hypothesis that signal(s) resulting from the absence of complex I, possibly mitochondrial ROS, induces AOX expression in CMSII. However, other signals
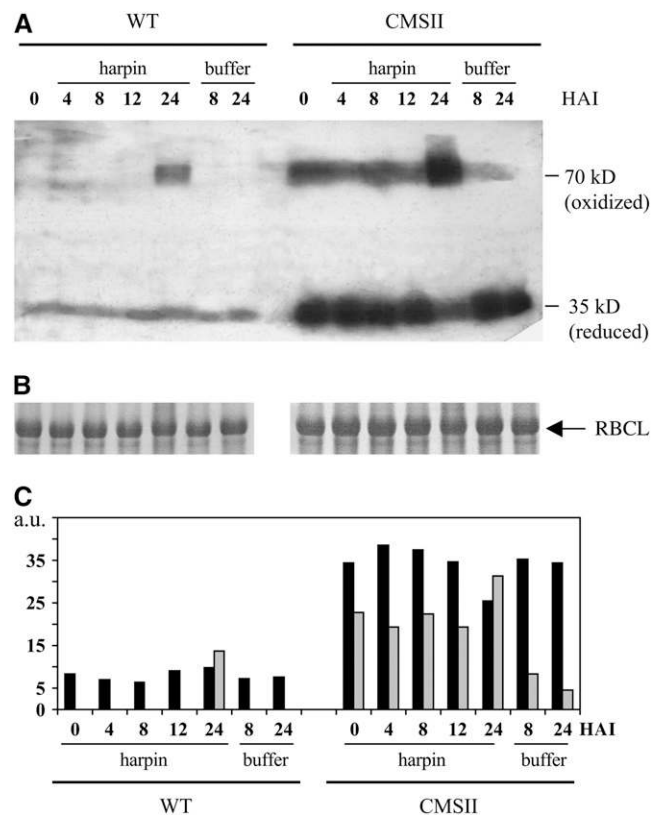

Figure 9. Immunoblots of AOX Protein from Wild-Type and CMSII Leaves during Harpin-Induced Cell Death.

Wild-type and CMSII leaf samples were harvested at different times after harpin (40 μg·mL^{-1}) or buffer infiltration into foliar tissues. Total leaf proteins were extracted as described in Methods.

(A) Immunodetection of reduced and oxidized forms of AOX. Leaf proteins (40 μg per lane) were separated by nonreducing SDS-PAGE on 12% acrylamide gels. After electrotransfer to nitrocellulose membranes, proteins were probed with *S. guttatum* anti-AOX antibody and detected by chemiluminescence. Reduced (35 kD) and oxidized (70 kD) forms of the AOX are indicated. Experiments were repeated three times with similar results, and a typical experiment is shown.

(B) Coomassie blue–stained gel showing protein loading; the 55-kD Rubisco large subunit (RBCL) is indicated.

(C) Quantification of oxidized and reduced forms of AOX. Reduced AOX, black bars; oxidized AOX, gray bars.
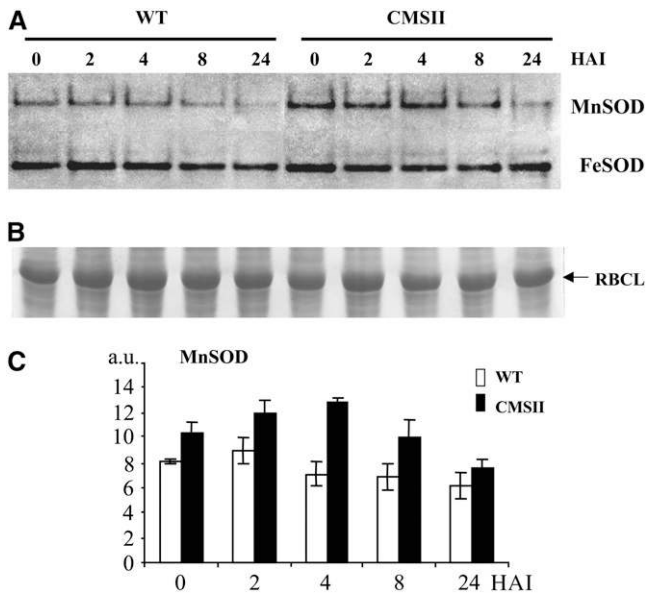
Figure 10. In-Gel Assay of SOD Activity during Harpin-Induced Cell Death.

Samples were harvested at different times (in hours) after harpin infiltration into wild-type or CMSII foliar tissues. Proteins (70 μg per lane) were extracted under nondenaturing conditions and were separated on a native 6 to 12% acrylamide gradient gel.

(A) Mitochondrial MnSOD and chloroplastic FeSOD activities were visualized on the same gel as described in Methods.

(B) Coomassie blue–stained gel showing protein loading; the 55-kD Rubisco large subunit (RBCL) is indicated.

(C) Histograms of MnSOD activities. In each genotype, values are means ± SE from eight different experiments for control leaves and three different experiments for harpin-elicited leaves. Differences between wild-type and CMSII values are significant at all times (P < 0.05), except at the 24-h time point. MnSOD activities were significantly lower for the pooled 8- to 24-HAI time points compared with the pooled 0- to 2-HAI time points.

may constrain AOX activity because of the need for ATP production in plants lacking the first coupling site. Whatever the exact mechanism(s) involved, the discrepancy between protein content and activity discussed above shows that, under physiological conditions, AOX is under tight control in plants with a defective energetic metabolism.

A Lower Induction of the AOX Pathway by Harpin in CMSII Than in Wild-Type Leaves

Leaf application of harpin induced a similar death process, as determined by visual observations and the kinetics of electrolyte leakage, in CMSII and wild-type leaves (Figure 5). The pattern of oxygen uptake measured in treated wild-type leaves was similar to that observed in the mutant (Figure 6). Oxygen uptake began to increase after 2 h, reached a transient maximum at 8 HAI, and was abolished after 48 h, showing the completion of the death process. These results clearly indicate a harpin-specific enhancement of mitochondrial respiration in inoculated leaves. The

increased mitochondrial activity precedes significant water loss (data not shown), electrolyte leakage, and the appearance of visible symptoms (Figure 5). The elevated respiration is therefore unlikely to be a consequence of the death process; instead, it may represent an early metabolic response to the elicitor.

In the wild type, the respiratory burst was essentially due to the fivefold induction of in vivo AOX activity (Figure 7). By contrast, COX activity increased by merely 50%. This rapid enhancement of AOX activity, 4 h after harpin inoculation, appeared to be mainly controlled by posttranslational mechanisms. Indeed, only a transient accumulation of AOX1 mRNA was observed, as previously reported (Garmier et al., 2002), preceding the increase in AOX activity. Moreover, an increase in AOX protein was observed only from 12 HAI. The enhanced level of oxidized AOX protein observed at 24 HAI (Figure 9) is in agreement with the altered cellular redox state at this time point, indicated by oxidation of ascorbate and glutathione (Figure 11). Taken together, these findings suggest the following feedback process in the wild-type plants. A harpin-induced oxidative burst, possibly dependent of plasmalemma NAD(P)H oxidase activity (Levine et al., 1994), transiently induces AOX gene expression, and this would be followed by posttranslational activation of the enzyme. In contrast with the results presented here, a marked increase in AOX expression/capacity has been reported in a number of plant/pathogen interactions (Lennon et al., 1997; Simons et al., 1999), including harpin (Xie and Chen, 2000; Boccara et al., 2001; Krause and Durner, 2004). However, to the best of our knowledge, an actual increase in AOX activity, as determined by oxygen isotope discrimination, has never been measured previously. For example, the infection of *Arabidopsis* plants with *Pseudomonas syringae* pv tomato led to an increase in total respiration and an induction of AOX transcripts and protein (Simons et al., 1999). However, the actual contribution of the AOX pathway to the observed respiratory enhancement was not determined. After infection of *N. tabacum* by TMV, neither respiration rates nor the partitioning of electrons were affected, despite an increase in the amount of AOX protein (Lennon et al., 1997). Our results for intact leaves contrast with those of Xie and Chen (2000), who reported an unchanged global respiration rate with inactivation of the COX pathway and ATP depletion in tobacco suspension cells after elicitation with harpin N_{Ea}. They also differ from the data of Krause and Durner (2004), who showed that harpin Z from *P. syringae* impaired mitochondrial functions in *Arabidopsis* cells. Similarly, cell death–inducing compounds, such as hydrogen peroxide and salicylic acid, have been reported to impair total respiration and the COX pathway in tobacco cell cultures (Robson and Vanlerberghe, 2002). The discrepancy between our results and those reported previously for suspension cells could result from inherent differences in metabolism between the photosynthetic tissues of green leaves reported here and suspension cells cultured in the dark that depend on external supply of carbohydrates for their survival.

The partitioning of electrons is markedly different in CMSII compared with the wild type. The harpin-induced respiratory elevation involved a twofold increase in both AOX and COX activities in the CMSII leaves, and the electron partitioning to the AOX pathway was actually twofold lower than in wild-type leaves. This shows that a more severe restriction of AOX occurs in the
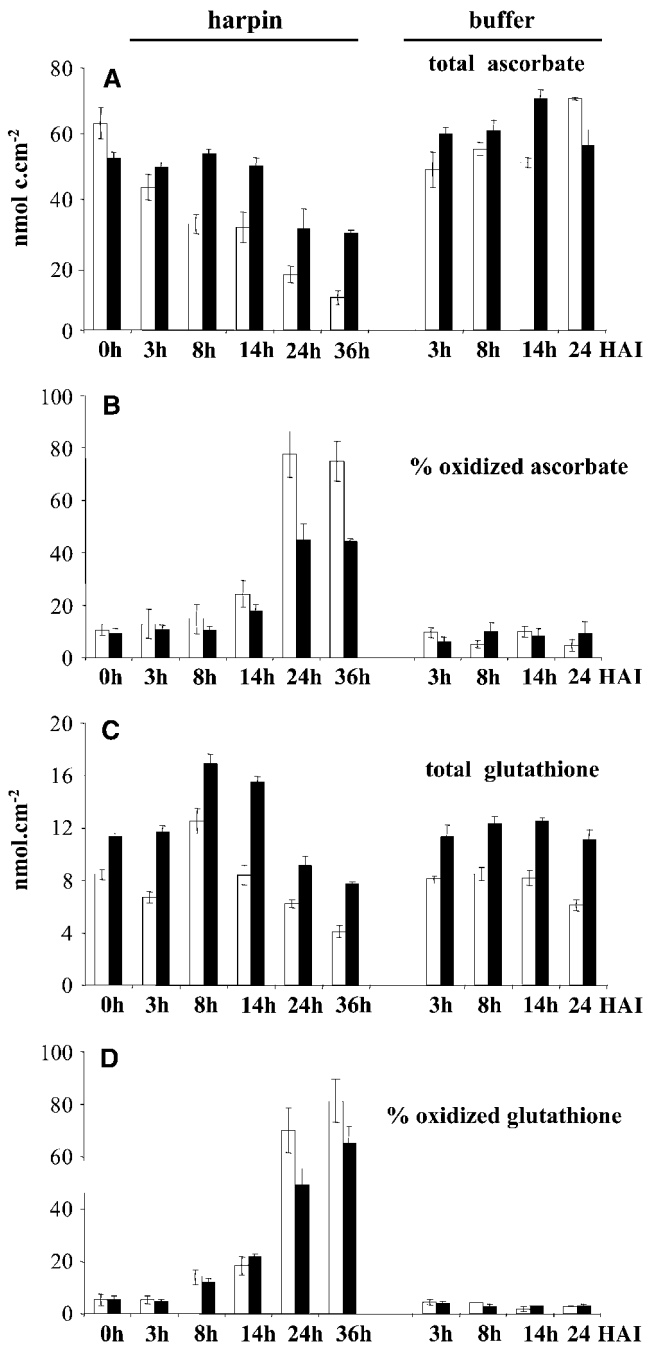
Figure 11. Ascorbate and Glutathione Content and Redox State in Harpin-Elicited Leaves.

Open bars, wild type; closed bars, CMSII. Values are the means ± SE from three independent experiments.

(A) Total ascorbate content expressed as nmol total ascorbate per cm^2 of leaf sample. The differences between the wild type and CMSII at 8 to 36 HAI are significant (P < 0.01).

(B) Percentage of oxidized ascorbate. Differences between the wild type and CMSII are significant (P < 0.01) for the time points 24 and 36 HAI.

(C) Total glutathione content expressed as nmol total glutathione per cm^2 of leaf sample. Differences between the wild type and CMSII are significant (P < 0.01) at all time points after harpin or buffer infiltration.

mutant under stress conditions than under nonstressed conditions. To estimate ATP production from the O_2 consumption data, we constructed a model derived from consensus stoichiometries of respiratory pathways (Table 3). Glucose produced by starch degradation (Lloyd, 2005) can be readily metabolized by respiration (Tcherkez et al., 2005), and sucrose from vacuolar storage is also a major substrate for dark respiration. Modeling ATP production based on the metabolism of sugars via standard glycolysis, TCA cycle, and the ETC for each combination of oxidase activities and plant genotype (i.e., accounting for decreased proton pumping via complex I in the mutant) demonstrated that ATP production was induced twofold during the first 8 HAI in both genotypes (Figure 7C). The similarity in ATP production between the genotypes strongly suggests that AOX/COX electron partitioning during the response to the elicitor is controlled to ensure an identical increase in ATP production. Work on isolated mitochondria has demonstrated the importance of the control of electron partitioning by ADP supply. An increase in ADP availability will decrease the proton motive force, thus allowing increased cytochrome pathway activity, as reviewed by Affourtit et al. (2001). Our results are consistent with previous in organello work (Sabar et al., 2000) and clearly suggest that a loss of proton pumping by complex I can be energetically compensated for by an increased respiratory electron transport activity and partitioning through the COX pathway, although with a higher carbon cost in respiration. This observation confirms the previous hypothesis that the CMSII phenotype is caused by perturbations in metabolite levels rather than an energetic deficiency (Dutilleul et al., 2003a, 2005). These results also further emphasize that future analyses of mitochondrial energy metabolism need to consider the more complex system with contributions by both proton pumping electron transport pathways and by direct ATP formation by glycolysis and the citric acid cycle.

Higher MnSOD Activity and Induction of Defense Reactions in CMSII Harpin-Elicited Leaves

In the wild type, the induction of AOX without any marked increase in COX activity would minimize superoxide generation during harpin-induced cell death. In CMSII, the significant relative induction of COX activity over AOX activity may lead to a higher generation of superoxide than in the wild type. In good agreement, mitochondrial MnSOD activity was higher in CMSII than in wild-type cells during the first 8 HAI (Figure 10). ROS, and especially hydrogen peroxide, act as crucial second messengers, especially in plant development and stress responses (Mittler, 2002; Foyer and Noctor, 2003). Their overproduction in harpin-elicited CMSII leaves could explain why the expression of genes encoding extramitochondrial enzymes, such as cytosolic ascorbate peroxidase and phenylalanine-ammonia lyase, are markedly more induced (Garmier et al., 2002). In addition, increased COX activity might contribute to improved antioxidant scavenging in CMSII leaves via ascorbate synthesis. Indeed, the final step of the

(D) Percentage of oxidized glutathione. Differences between the wild type and CMSII are significant (P < 0.01) for the time points 24 and 36 HAI.

synthesis of ascorbate, the major nonenzymatic antioxidant of plant cells (Noctor and Foyer, 1998), resides in the mitochondria and is linked to respiratory fluxes between complexes III and IV (Bartoli et al., 2000; Millar et al., 2003). The rapid ascorbate depletion witnessed in the wild-type leaves after harpin elicitation is not observed in CMSII until 24 HAI (Figure 11). Moreover, the harpin-induced increase in glutathione observed during the first 8 HAI is higher in CMSII leaves than in wild-type leaves, in good agreement with the view that antioxidant defense is better in CMSII leaves (Dutilleul et al., 2003b). Most importantly, the oxidation state of the leaf ascorbate and glutathione pools, which reflects the extent of oxidation experienced in the elicited cells (Noctor and Foyer, 1998), is delayed in CMSII (Figure 11), even at the end of the process, when cell death has taken place (Figure 5). Taken together, these results indicate that both mitochondrial and extramitochondrial antioxidant responses are more induced in CMSII than in wild-type harpin-infiltrated leaves.

Respiratory Pathways, Mitochondrial ROS, Defense Responses, and Cell Death: Where Is the Causal Link?

An increased AOX activity in wild-type harpin-elicited leaves is intriguing in view of its accepted role in controlling overreduction of the respiratory chain and subsequent generation of ROS that are considered as key second messengers in stress responses. On the other hand, a role for AOX might be viewed as a compartment-specific defense system to preserve mitochondrial integrity and functioning. Accordingly, the modeling of oxidative phosphorylation based on actual respiratory fluxes indicated the same marked increase in ATP production in both the wild type and CMSII. Although this increase remains to be shown directly, these data strongly suggest that ATP availability might be an important factor in the execution of harpin-induced cell death. In good agreement, the plant HR is generally considered to be an active process (He et al., 1994), similar to the ATP-dependent apoptosis of animal cells (Nieminen, 2003). By contrast, although mitochondrial ROS are likely to activate defense responses, they could not be directly involved in cell death or even could counteract the process. Interestingly, it has been recently shown that ROS generated by plasmalemma NAD(P)H activity impair the spread of cell death in *Arabidopsis* (Torres et al., 2005). In wild-type *N. sylvestris* leaves, AOX and COX activities would be finely adjusted to allow an appropriate balance between ATP and mitochondrial ROS generation during harpin elicitation. This balance could be altered in CMSII leaves, where the different partitioning to respiratory routes might be expected to generate more mitochondrial ROS than in the wild type. This would explain the overexpression of antioxidant and defense genes (Garmier et al., 2002), the delayed oxidation of total ascorbate and gluthatione pools (Figure 11), and the altered response at the whole-cell level (Boccara et al., 2001). Both intra- and extramitochondrial antioxidant defenses might also be involved in the enhanced stress tolerance of CMSII plants to ozone and TMV (Dutilleul et al., 2003b).

It is clear that two different strategies are used by wild-type and CMSII plants in response to harpin elicitation. However, this results in a similar timing and extent of in planta cell death under the experimental conditions of this study. Experiments are in progress to evaluate whether different factors, such as elicitor dose, plant age, and environmental conditions, might differentially modulate the response of both genotypes to harpin.

METHODS

Plant Material

The mitochondrial CMSII mutant was obtained from *Nicotiana sylvestris* wild-type protoplast cultures (Li et al., 1988) and maintained by backcrossing with wild-type plants as a male donor. Except otherwise stated, plants were grown in the Institut de Biotechnologie des Plantes greenhouses under a 16-h photoperiod. Natural light was supplemented by artificial lighting to give a minimum of 400 μmol m^{-2} s^{-1} during the day period, at day/night temperatures of 23.5/17.5°C and day/night relative humidity of 70/60%. Plants were fed with Hydrokani C2 nutritive solution. For oxygen discrimination measurements (see below), plants were grown in the greenhouses of the University de les Illes Balears under natural light and watered every 2 d with tap water. Half-strength Hoagland solution (Epstein, 1972) was applied every 5 d. Three days before respiration and oxygen isotope fractionation measurements, plants were placed in a growth chamber at 25°C at a light intensity of 600 μmol m^{-2} s^{-1}.

Harpin Production and Inoculation

Harpin was produced as described by Gaudriault et al. (1998). Solutions of 40 μg·mL^{-1} harpin in 10 mM Tris-HCl, pH 7.5, and 0.1 mM EDTA buffer were infiltrated into leaf tissues with a syringe without a needle, as described by Garmier et al. (2002). Mock infiltration of buffer was performed as a control by the same procedure on different plants. Samples were punched out with a core-borer (1.5 cm in diameter, unless otherwise specified). The second fully developed leaf of 6-week-old wild-type and 2-month-old CMSII plants were used to compare plants at the same developmental stage. In all experiments, careful controls were performed to ensure that the infiltrated zone was actually undergoing cell death. To determine this point, we measured the following features at the 24-h time point: (1) the immediate area outside the harvested zone (Figure 5); (2) a comparable infiltration site on the same leaf was not harvested, ensuring that the whole area was fully necrotic. Experiments that did not meet these two criteria were dismissed.

Electrolyte Leakage Measurements

Electrolyte leakage was measured as described by Pike et al. (1998) using a conductivity meter (CD60; Solea-Tacussel). At different times after harpin or buffer infiltration, eight discs (2.5 cm^2 in total) were punched out from treated tissues with a cork-borer and placed in 10 mL of sterile distilled water. Vials were incubated at least 2 h under continuous stirring at 20°C.

RNA Isolation and Gel Blot Analysis

Total RNA was extracted by the Trizol (Gibco BRL) procedure from mature leaf pieces harvested from 2-month-old plants after 10 h of illumination, as described by Dutilleul et al. (2003b). RNA gel blot analyses were performed on 12 μg of total RNA using a 380-bp *N. sylvestris* cDNA, 100% homologous to the internal region of *Nicotiana tabacum AOX1* (Sabar et al., 2000) and *N. sylvestris atp9* and *coxI* mitochondrial sequences as probes (Brangeon et al., 2000).

Purification of Leaf Mitochondria

Mitochondrial preparations were as described by Sabar et al. (2000). Briefly, freshly harvested leaves of 3-month-old plants were

homogenized in 0.6 M mannitol, 40 mM MOPS, pH 7.5, 0.6% insoluble polyvinylpyrrolidone, 3 mM EGTA, 4 mM cysteine, and 0.5% BSA. After filtration through a 30-μm mesh, the juice was centrifuged at 900g for 7 min. The supernatant was centrifuged at 10,000g for 15 min and the pellet resuspended in 0.6 M mannitol, 10 mM MOPS, pH 7.2, and 0.1% BSA. Washed mitochondria were obtained after a second cycle of centrifuga- tion and then purified on a self-forming 32% (v/v) Percoll gradient (Pharmacia). In some experiments, 5 mM pyruvate was added to all buffers during the mitochondrial isolation process. Purified mitochondria were resuspended in the washing buffer, supplemented ($+$) or not ($-$) with 20 mM citrate, incubated for 1 h at room temperature, and then pelleted by centrifugation as described by Vanlerberghe et al. (1995).

Total Protein Extraction

Leaf discs were ground in liquid nitrogen, and total proteins were extracted in 2$\times$ Laemmli buffer, with or without 0.2% β-mercaptoethanol. The extract was centrifuged for 10 min at 20,000g to eliminate insoluble material, and protein was determined according to Bradford (1976).

In-Gel Determination of SOD Activity

Leaf disks were ground in liquid nitrogen and extraction buffer (0.1 M Tris- HCl, pH 8.1, 10% sucrose, 0.5 mM Pefabloc protease inhibitor [Fluka], and 0.2% β-mercaptoethanol). Extracts were cleared by centrifugation for 5 min at 20,000g. The supernatant was kept, and debris was pelleted by centrifugation for 30 min at 150,000g. Supernatants were frozen at -20°C. The entire extraction procedure was performed at 4°C. Sam- ples containing 70 μg proteins in nondenaturing Laemmli buffer were separated on 12 to 6% polyacrylamide gels at 4°C. SOD activities were visualized using the in situ staining technique of Beauchamp and Fridovitch (1971). After 30 min of dark incubation with a mixture contain- ing Nitro Blue Tetrazolium, gels were placed in the light for 30 min. SOD activity caused achromatic zones on otherwise uniformly blue-stained gels. The different SOD isoforms were characterized by inhibitor treat- ments before staining, KCN inhibiting Cu/ZnSODs, and H_2O_2 inhibiting both FeSOD and Cu/ZnSOD activities (data not shown).

Immunoblot Analysis

Unless otherwise specified in the figure legend, total leaf proteins and mitochondrial proteins were separated on 12% (w/v) acrylamide gels by either reducing or nonreducing SDS-PAGE using SDS Tris-Gly buffer and electroblotted to nitrocellulose membrane in Tris-Gly buffer and 20% (v/v) methanol. Membranes were blocked with 5% skimmed, nonfat milk and probed with a monoclonal antibody against *S. guttatum* AOX (Elthon et al., 1989) and antisera against control proteins. Horseradish peroxidase– conjugated anti-mouse IgG was used as a secondary antibody at a di- lution of 1:2500, and immune complex was visualized by ECL according to manufacturer's instructions (Roche Diagnostics).

Ascorbate and Glutathione Determinations

Leaf discs were harvested and ground in liquid nitrogen and then in 1 mL of 1 M $HClO_4$. On thawing, samples were then centrifuged for 15 min at 15,000g and 4°C. The pH of the clarified supernatant was adjusted to 5.6 with K_2CO_3 and insoluble $KClO_4$ removed by centrifugation. Ascorbate and glutathione were measured in the same supernatant. Total and reduced ascorbate contents were measured as the ascorbate oxidase– dependent decrease in A_{265}, before (reduced ascorbate) and after (total ascorbate) treatment of the sample for 15 min with 0.1 M DTT (modified from Foyer et al., 1983). The 1-mL reaction mixture contained 0.12 M NaH_2PO_4, pH 5.6, and 0.1 mL extract. The difference in OD before and after addition of 1 unit of ascorbate oxidase was converted to ascorbate concentration ($\varepsilon_{265} = 12.6$ mM^{-1}cm^{-1}). Total and oxidized glutathione contents were measured using the enzymatic recycling assay involving the NADPH-driven glutathione-dependent reduction of 5,5-dithiobis 2-nitro-benzoic acid at 412 nm (Noctor and Foyer, 1998).

Respiratory Measurements on Intact Tissues with a Gas Phase Dual-Inlet System

V_t, v_{cyt}, and v_{alt} in leaves were determined using a closed gas phase system connected to a dual-inlet mass spectrometer as previously de- scribed (Gaston et al., 2003) with minor changes as described below. The measuring system consisted of a 4-mL closed cuvette where the plant tissue was placed and from which 200 μL of air was sequentially with- drawn and fed into the mass spectrometer sample bellows. The isotope ratio mass spectrometer (Thermo Scientific) simultaneously analyzed mass-to-charge ratios of 32 ($^{16}O_2$), 34 ($^{18}O^{16}O$), and 28 (N_2) operating in dual-inlet mode and by comparison with a standard air sample. The stainless steel cuvette was equipped with two inlets: one connected to a 5-mL air-tight syringe and the other to the mass spectrometer sample bellows through a capillary tube with a pneumatically controlled on–off microneedle valve. The sampled air went trough a liquid N_2 trap for water and CO_2 removal. To avoid any drop in cuvette pressure during the experiment, the air was mixed using an air-tight syringe, which was initially left with 1 mL of air. During the experiment, the syringe was used to mix the air. At the beginning of every measurement, 200 μL of the syringe was placed in the cuvette to maintain its atmospheric pressure. The system was regularly tested for leaks by filling the cuvette with He and measuring the sample over three times the experimental time span. No oxygen signals were observed. The time between successive samples was 12 min, and the length of each full experiment varied between 60 and 90 min.

One or two leaf samples (5.1 cm^2 each) were placed in the 4-mL stainless cuvette. All experiments were performed at a controlled tem- perature of 23°C. For inhibitory treatments used to measure fractionation values through each pathway, leaf discs were kept in 5 mM KCN (in water) for 30 min with constant shaking. For SHAM, we used 100 mL of 10 mM solution in a beaker, and the tobacco leaf was placed in the SHAM solution under illumination. No recovery from inhibitor treat- ment was observed as respiratory rates and oxygen isotope fractionation remained constant throughout the experiment. All stocks were freshly prepared before measurement. Calculations of the oxygen isotopic fractionation were made as described by Guy et al. (1989) and Ribas- Carbo et al. (1995) without argon correction. The electron partitioning between the two pathways in the absence of inhibitors was calculated as described by Guy et al. (1989) without forcing the slope to intercept the origin. Over the course of the experiment, leaf samples consumed a maximum of 10% of the initial oxygen (21%). r^2 values of all unconstrained linear regression between $-\ln f$ and $\ln(R/R_o)$ (with at least five data points) were at least 0.995, corresponding to an error in the estimation of <0.5% (Ribas-Carbo et al., 1995; Lennon et al., 1997).

The electron partitioning through the alternative pathway (τ_a) was calculated as follows:

$$\tau_a = (\Delta_n - \Delta_c)/(\Delta_a - \Delta_c),$$

where Δ_n, Δ_c, and Δ_a are the isotope fractionation in the absence of inhibitors, in the presence of SHAM, and in the presence of KCN, respectively. The individual activities of the COX (v_{cyt}) and the AOX alternative pathway (v_{alt}) were obtained from multiplying the total oxygen uptake (V_{tot}) by the partitioning to each pathway as follows:

$$v_{cyt} = V_{tot} \times (1 - \tau_a)$$

$$v_{alt} = V_{tot} \times \tau_a.$$

Modeling ATP Production

Modeling of ATP production was performed by theoretically calculating ATP/O_2 values for each combination of catabolic reaction (e.g., glucose via standard glycolysis and TCA cycle), plant genotype, and oxidase pathway. The ATP/O_2 stoichiometries were then used to convert O_2 consumption to ATP production. Consensus values of oxidative phosphorylation stoichiometries were used: NADH-O_2 (via complex I and COX), 10 H$^+$/2e$^-$; NADH-O_2 (via external or internal alternative NADH dehydrogenase and COX), 6 H$^+$/2e$^-$; NADH-O_2 (via complex I and AOX), 4 H$^+$/2e$^-$; NADH-O_2 (via external NADH dehydrogenase and AOX), 2 H$^+$/2e$^-$; NADH-O_2 (via internal NADH dehydrogenase and AOX), 0 H$^+$/2e$^-$; succinate-O_2 (via SDH and COX), 6 H$^+$/2e$^-$; succinate-O_2 (via SDH and AOX), 0 H$^+$/2e$^-$; ATP synthesis and export, 4 H$^+$/ATP (Nicholls and Ferguson, 2002; Browse et al., 2006). The stoichiometry of proton pumping by the pathway from external NADH via AOX was derived theoretically, but it has also been observed in organello (Glaser et al., 1998). These values were combined with stoichiometries of Glc degradation via the standard glycolysis and TCA cycle pathways, shown here as ATP/Glc, which equals 6 times ATP/O_2. For malate, the factor is 3. The model assumes a partitioning of matrix NADH between complex I and the alternative internal NADH dehydrogenase of 80:20 in the wild type and a distribution of electrons between internal and external NADH dehydrogenase in the CMSII complex I mutant of 50:50. Engagement of the external NADH oxidation would involve the export of reductant via the malate shuttle and is supported by the strongly elevated activity levels of the external NADH dehydrogenase in CMSII mitochondria (Sabar et al., 2000). Pearson correlation coefficients were calculated using SPSS 11 for Macintosh.

Quantification and Statistical Analyses

Relative signal intensities were quantified using Scion Image Beta 4.02 Win. Analysis of variance statistical analysis was performed with STATISTICA software (STATSOFT).

Accession Number

Sequence data from this article can be found in the GenBank/EMBL data libraries under accession number S71335 (*N. tabacum AOX1*).

REFERENCES

Affourtit, C., Krab, K., and Moore, A.L. (2001). Control of plant mitochondrial respiration. Biochim. Biophys. Acta **1504:** 58–69.

Andersson, M.E., and Nordlund, P. (1999). A revised model of the active site of alternative oxidase. FEBS Lett. **449:** 19–22.

Bartoli, C.G., Pastori, G.M., and Foyer, C.H. (2000). Ascorbate biosynthesis in mitochondria is linked to the electron transport chain between complexes III and IV. Plant Physiol. **123:** 335–344.

Beauchamp, C., and Fridovitch, I. (1971). Superoxide dismutase: Improved assays and an assay applicable to acrylamide gels. Anal. Biochem. **44:** 276–287.

Boccara, M., Boué, C., Garmier, M., De Paepe, R., and Boccara, A.C. (2001). Infra-red thermography revealed a role for mitochondria in pre-symptomatic cooling during harpin-induced hypersensitive response. Plant J. **28:** 663–670.

Bradford, M. (1976). A rapid and sensitive method for the quantitation of microgram quantities of protein utilizing the principle of protein-type binding. Anal. Biochem. **7:** 248–254.

Brangeon, J., Sabar, M., Gutierres, S., Combettes, B., Bove, J., Gendy, C., Chétrit, P., Des Francs-Small, C.C., Pla, M., Vedel, F., and De Paepe, R. (2000). Defective splicing of the first *nad4* intron is associated with lack of several Complex I subunits in the *Nicotiana sylvestris* NMS1 nuclear mutant. Plant J. **21:** 269–280.

Browse, J., Møller, I.M., and Rasmusson, A.G. (2006). Respiration and lipid metabolism. In Plant Physiology, 4th ed., L. Taiz and E. Zeiger, eds (Sunderland, MA: Sinauer Associates), pp. 253–288.

Chétrit, P., Rios, R., De Paepe, R., Vitart, V., Li, X.Q., and Vedel, F. (1992). Cytoplasmic male sterility is associated with large deletions in the mitochondrial DNA of two *Nicotiana sylvestris* protoclones. Curr. Genet. **21:** 131–137.

Clifton, R., Millar, A.H., and Whelan, J. (2006). Alternative oxidases in Arabidopsis: A comparative analysis of differential expression in the gene family provides new insights into function of non-phosphorylating bypasses. Biochim. Biophys. Acta **1757:** 730–741.

Considine, M.J., Holtzapffel, R.C., Day, D.A., Whelan, J., and Millar, A.H. (2002). Molecular distinction between alternative oxidase from monocots and dicots. Plant Physiol. **129:** 949–953.

Day, D.A., Krab, K., Lambers, H., Moore, A.L., Siedow, J.N., Wagner, A.M., and Wiskich, J.T. (1996). The cyanide resistant oxidase: To inhibit or not to inhibit, that is the question. Plant Physiol. **110:** 1–2.

Day, D.A., Millar, A.H., Wiskich, J.T., and Whelan, J. (1994). Regulation of alternative oxidase activity by pyruvate in soybean mitochondria. Plant Physiol. **106:** 1421–1427.

De Paepe, R., Forchioni, A., Chétrit, P., and Vedel, F. (1993). Specific mitochondrial proteins in pollen: Presence of an additional ATP synthase β subunit. Proc. Natl. Acad. Sci. USA **90:** 5934–5938.

Dutilleul, C., Driscoll, S., Cornic, G., De Paepe, R., Foyer, C., and Noctor, G. (2003a). Functional mitochondrial complex I is required by tobacco leaves for optimal photosynthetic performance in respiratory conditions and during transients. Plant Physiol. **131:** 264–275.

Dutilleul, C., Garmier, M., Noctor, G., Mathieu, C., Chétrit, P., Foyer, C., and De Paepe, R. (2003b). Leaf mitochondria modulate whole cell redox homeostasis, set antioxidant capacity, and determine stress resistance through altered signaling and diurnal regulation. Plant Cell **15:** 1212–1226.

Dutilleul, C., Lelarge, C., Prioul, J.L., De Paepe, R., Foyer, C.H., and Noctor, G. (2005). Mitochondria-driven changes in leaf NAD status exert a crucial influence on the control of nitrate assimilation and the integration of carbon and nitrogen metabolism. Plant Physiol. **139:** 64–78.

Elthon, T.E., Nickels, R.L., and McIntosh, L. (1989). Monoclonal antibodies to the alternative oxidase in higher plant mitochondria. Plant Physiol. **89:** 1311–1317.

Epstein, E. (1972). Mineral Nutrition of Plants: Principles and Perspectives. (New York: John Wiley & Sons).

Foyer, C.H., and Noctor, G. (2003). Redox sensing and signaling associated with reactive oxygen in chloroplasts, peroxisomes and mitochondria. Physiol. Plant 119: 355–364.

Foyer, C.H., Rowell, J., and Walker, D. (1983). Measurement of the ascorbate content of spinach leaf protoplasts and chloroplasts during illumination. Planta 157: 239–244.

Garmier, M., Dutilleul, C., Mathieu, C., Chétrit, P., Boccara, M., and De Paepe, R. (2002). Changes in antioxidant expression and harpin-induced hypersensitive response in a Nicotiana sylvestris mitochondrial mutant. Plant Physiol. Biochem. 40: 561–566.

Gaston, S., Ribas-Carbo, M., Busquets, S., Berry, J.A., Zabalza, A., and Royulea, M. (2003). Changes in mitochondrial electron partitioning in response to herbicides inhibiting branched-chain amino acid biosynthesis in soybean. Plant Physiol. 133: 1351–1359.

Gaudriault, S., Brisset, M.N., and Barny, M.A. (1998). HrpW of Erwinia amylovora, a new Hrp-secreted protein. FEBS Lett. 428: 224–228.

Glaser, E., Sjöling, S., Tanudji, M., and Whelan, J. (1998). Mitochondrial protein import in plants. Plant Mol. Biol. 38: 311–338.

Gonzalez-Meler, M.A., Giles, L., Thomas, R.B., and Siedow, J.N. (1999). Metabolic regulation of leaf respiration and alternative pathway activity in response to phosphate supply. Plant Cell Environ. 24: 205–215.

Gutierres, S., Sabar, M., Lelandais, C., Chétrit, P., Diolez, P., Degand, H., Boutry, M., Vedel, F., de Kouchkovsky, Y., and De Paepe, R. (1997). Lack of mitochondrial and nuclear-encoded subunits of complex I and alteration of the respiratory chain in Nicotiana sylvestris mitochondrial deletion mutants. Proc. Natl. Acad. Sci. USA 94: 3436–3441.

Guy, R.D., Berry, J.A., Fogel, M.L., and Hoering, T.C. (1989). Differential fractionation of oxygen isotopes by cyanide-resistant and cyanide-sensitive respiration in plants. Planta 177: 483–491.

He, S.Y., Bauer, D.W., Collmer, A., and Beer, S.V. (1994). Hypersensitive response elicited by Erwinia amylovora harpin requires active plant metabolism. Mol. Plant Microbe Interact. 7: 289–292.

Juszczuk, I.M., Wagner, A.M., and Rychter, A.M. (2001). Regulation of alternative oxidase activity during phosphate deficiency in bean roots (Phaseolus vulgaris). Physiol. Plant 113: 185–192.

Karpova, O.V., Kuzmin, E.V., Elthon, T.E., and Newton, K.J. (2002). Differential expression of alternative oxidase genes in maize mitochondrial mutants. Plant Cell 14: 3271–3284.

Krause, M., and Durner, J. (2004). Harpin inactivates mitochondria in Arabidopsis suspension cells. Mol. Plant Microbe Interact. 17: 131–139.

Lambers, H. (1982). Cyanide resistant respiration: A non-phosphorylating electron transport pathway acting as an energy overflow. Physiol. Plant 55: 478–485.

Lelandais, C., Albert, B., Gutierres, S., De Paepe, R., Godelle, B., Vedel, F., and Chétrit, P. (1998). Organization and expression of the mitochondrial genome in the Nicotiana sylvestris CMSII mutant. Genetics 150: 873–882.

Lennon, A.M., Neuenschwander, U.H., Ribas-Carbo, M., Giles, L., Ryals, J.A., and Siedow, J.N. (1997). The effects of salicylic acid and tobacco mosaic virus infection on the alternative oxidase of tobacco. Plant Physiol. 115: 783–791.

Lennon, A.M., Pratt, J., Leach, G., and Moore, A.L. (1995). Developmental regulation of respiratory activity in pea leaves. Plant Physiol. 107: 925–932.

Levine, A., Tenhaken, R., Dixon, R., and Lamb, C. (1994). H_2O_2 from the oxidative burst orchestrates the plant hypersensitive disease resistance response. Cell 79: 583–593.

Li, X.Q., Chétrit, P., Mathieu, C., Vedel, F., De Paepe, R., Rémy, M., and Ambard-Bretteville, F. (1988). Regeneration of cytoplasmic male sterile protoclones of Nicotiana sylvestris with mitochondrial variation. Curr. Genet. 13: 261–266.

Lloyd, J.R. (2005). Leaf starch degradation comes out of the shadows. Trends Plant Sci. 10: 130–137.

Maxwell, D.P., Wang, Y., and McIntosh, L. (1999). The alternative oxidase lowers mitochondrial reactive oxygen production in plant cells. Proc. Natl. Acad. Sci. USA 96: 8271–8276.

Meeuse, B.J.D. (1975). Thermogenic respiration in aroids. Annu. Rev. Plant Physiol. 26: 117–126.

Michalecka, A.M., Agius, S.R., Møller, I.M., and Rasmusson, A.G. (2004). Identification of a mitochondrial external NADPH dehydrogenase by overexpression in transgenic Nicotiana sylvestris. Plant J. 37: 415–425.

Millar, A.H., Hoefnagel, M.H.N., Day, D.A., and Wiskich, J.T. (1996). Specificity of the organic acid activation of alternative oxidase in plant mitochondria. Plant Physiol. 111: 613–618.

Millar, A.H., Mittova, V., Kiddle, G., Heazlewood, J.L., Bartoli, C.G., Theodoulou, F.L., and Foyer, C.H. (2003). Control of ascorbate synthesis by respiration and its implications for stress responses. Plant Physiol. 133: 443–447.

Millar, A.H., Wiskich, J.T., Whelan, J., and Day, D.A. (1993). Organic acid activation of the alternative oxidase of plant mitochondria. FEBS Lett. 329: 259–262.

Millenaar, F.F., Gonzalez-Meler, M.A., Fiorani, F., Welschen, R., Ribas-Carbo, M., Siedow, J.N., Wagner, A.M., and Lambers, H. (2001). Regulation of alternative oxidase activity in six wild monocotyledonous species. An in vivo study at the whole root level. Plant Physiol. 126: 376–387.

Millenaar, F.F., Gonzalez-Meler, M.A., Siedow, J.N., Wagner, A.M., and Lambers, H. (2002). Role of sugars and organic acids in regulating the concentration and activity of the alternative oxidase in Poa annua roots. J. Exp. Bot. 53: 1081–1088.

Mittler, R. (2002). Oxidative stress, antioxidants and stress tolerance. Trends Plant Sci. 7: 405–410.

Møller, I.M. (2001). Plant mitochondria and oxidative stress: Electron transport, NADPH turnover and metabolism of reactive oxygen species. Annu. Rev. Plant Physiol. Plant Mol. Biol. 52: 561–591.

Nicholls, D.G., and Ferguson, S.J. (2002). Bioenergetics 3. (Amsterdam: Academic Press).

Nieminen, A. (2003). Apoptosis and necrosis in health and disease: Role of mitochondria. Int. Rev. Cytol. 224: 29–55.

Noctor, G., and Foyer, C.H. (1998). Ascorbate and glutathione: Keeping active oxygen under control. Annu. Rev. Plant Physiol. Plant Mol. Biol. 49: 249–279.

Ordog, S.H., Higgins, V.J., and Vanlerberghe, G.C. (2002). Mitochondrial alternative oxidase is not a critical component of plant viral resistance but may play a role in the hypersensitive response. Plant Physiol. 121: 1309–1320.

Parsons, H.L., Yip, J.Y.H., and Vanlerberghe, G.C. (1999). Increased respiratory restriction during phosphate-limited growth in transgenic tobacco cells lacking alternative oxidase. Plant Physiol. 121: 1309–1320.

Pike, S.M., Adam, A.L., Pu, X.A., Hoyos, M.E., Laby, R., Beer, S.V., and Novacky, A. (1998). Effects of Erwinia amylovora harpin on tobacco leaf cell membranes are related to leaf necrosis and electrolyte leakage and distinct from perturbations caused by inoculated E. amylovora. Physiol. Mol. Plant Pathol. 53: 39–60.

Pineau, B., Mathieu, C., Gérard-Hirne, C., De Paepe, R., and Chétrit, P. (2005). Targeting the NAD7 subunit to mitochondria restores a functional complex I and a wild type phenotype in the Nicotiana sylvestris CMSII mutant lacking nad7. J. Biol. Chem. 28: 25994–26001.

Pla, M., Mathieu, C., De Paepe, R., Chétrit, P., and Vedel, F. (1995). Deletion of the last two exons of the mitochondrial *nad7* gene results in lack of the NAD7 polypeptide in a *Nicotiana sylvestris* CMS mutant. Mol. Gen. Genet. **248:** 79–88.

Purvis, A.C. (1997). Role of the alternative oxidase in limiting superoxide production by plant mitochondria. Physiol. Plant **100:** 165–170.

Purvis, A.C., and Shewfelt, R.L. (1993). Does the alternative pathway ameliorate chilling injury in sensitive plant tissues? Physiol. Plant **88:** 712–718.

Rasmusson, A.G., Heiser, V.V., Zabaleta, E., Brennicke, A., and Grohmann, L. (1999). Homologues of yeast and bacterial rotenone-insensitive NADH dehydrogenases in higher eukaryotes: Two enzymes are present in potato mitochondria. Plant J. **20:** 79–88.

Rasmusson, A.G., Soole, K.L., and Elthon, T.E. (2004). Alternative NAD(P)H dehydrogenases of plant mitochondria. Annu. Rev. Plant Biol. **55:** 23–39.

Rhoads, D.M., Umbach, A.L., Sweet, C.R., Lennon, A.M., Rauch, G.S., and Siedow, J.N. (1998). Regulation of the cyanide-resistant alternative oxidase of plant mitochondria: Identification of the cysteine involved in alpha-keto acid stimulation and intersubunit disulfide bond formation. J. Biol. Chem. **273:** 30750–30756.

Ribas-Carbo, M., Aroca, R., Gonzales-Meler, M.A., Irigoyen, J., and Sanchez-Diaz, M. (2000). The electron partitioning between the cytochrome and alternative respiratory pathways during chilling recovery in two cultivars of maize differing in chilling sensitivity. Plant Physiol. **122:** 199–204.

Ribas-Carbo, M., Berry, J.A., Yakir, D., Giles, L., Robinson, S.A., Lennon, A.M., and Siedow, J.N. (1995). Electron partitioning between the cytochrome and alternative pathways in plant mitochondria. Plant Physiol. **109:** 829–837.

Ribas-Carbo, M., Lennon, A.M., Robinson, S.A., Giles, L., Berry, J.A., and Siedow, J.N. (1997). The regulation of the electron partitioning between the cytochrome and alternative pathways in soybean cotyledon and root mitochondria. Plant Physiol. **113:** 903–911.

Ribas-Carbo, M., Robinson, S.A., and Gilles, L. (2005a). The application of the oxygen-isotope technique to assess respiratory pathway partitioning. In Plant Respiration: From Cell to Ecosystem, Advances in Photosynthesis and Respiration, Vol. 18, H. Lambers and M. Ribas-Carbo, eds (Dordrecht, The Netherlands: Springer-Verlag), pp. 31–42.

Ribas-Carbo, M., Taylor, N.L., Gilles, L., Busquets, S., Finnegan, P.M., Day, D.A., Lambers, H., Medrano, H., Berry, J.A., and Flexas, J. (2005b). Effects of water stress on respiration in soybean leaves. Plant Physiol. **139:** 466–473.

Robinson, S.A., Ribas-Carbo, M., Yakir, D., Giles, L., Reuveni, Y., and Berry, J.A. (1995). Beyond SHAM and cyanide: Opportunities for studying the alternative oxidase in plant respiration using oxygen isotope discrimination. Aust. J. Plant Physiol. **22:** 487–496.

Robinson, S.A., Yakir, D., Ribas-Carbo, M., Giles, L., Osmond, B., Siedow, J.N., and Berry, J.A. (1992). Measurements of the engagement of the cyanide-resistant respiration in the crassulacean acid metabolism plant *Kalanchoe daigremontania* with the use of on-line oxygen isotope discrimination. Plant Physiol. **100:** 1087–1091.

Robson, C.A., and Vanlerberghe, G.C. (2002). Transgenic plant cells lacking mitochondrial alternative oxidase have increased susceptibility to mitochondria-dependent and -independent pathways of programmed cell death. Plant Physiol. **129:** 1908–1920.

Sabar, M., De Paepe, R., and de Kouchkovsky, Y. (2000). Complex I impairment, respiratory compensation and photosynthetic decrease in nuclear and mitochondrial male sterile mutants of *Nicotiana sylvestris.* Plant Physiol. **124:** 1239–1249.

Saisho, D., Nambara, E., Naito, S., Tsutsumi, N., Hirai, A., and Nakazono, M. (1997). Characterization of the gene family for alternative oxidase from *Arabidopsis thaliana.* Plant Mol. Biol. **35:** 585–596.

Simons, B.H., Millenaar, F.F., Mulder, L., Van Loon, L.C., and Lambers, H. (1999). Enhanced expression and activation of the alternative oxidase during infection of *Arabidopsis* with *Pseudomonas syringae* pv tomato. Plant Physiol. **120:** 529–538.

Tcherkez, G., Cornic, G., Bligny, R., Gout, E., and Ghashghaie, J. (2005). *In vivo* respiratory metabolism of illuminated leaves. Plant Physiol. **138:** 1596–1606.

Torres, M.A., Jones, J.D., and Dangl, J.L. (2005). Pathogen-induced, NADPH oxidase-derived reactive oxygen intermediates suppress spread of cell death in *Arabidopsis thaliana.* Nat. Genet. **37:** 1130–1134.

Umbach, A.L., Ng, V.S., and Siedow, J.N. (2006). Regulation of plant alternative oxidase activity: A tale of two cysteines. Biochim. Biophys. Acta **1757:** 135–142.

Umbach, A.L., and Siedow, J.N. (1993). Covalent and noncovalent dimers of the cyanide-resistant alternative oxidase protein in higher plant mitochondria and their relationships to enzyme activity. Plant Physiol. **103:** 845–854.

Umbach, A.L., and Siedow, J.N. (1996). The reaction of the soybean cotyledon mitochondrial cyanide-resistant oxidase with sulfhydryl reagents suggests that α-keto acids activation involves the formation of a thiohemiacetal. J. Biol. Chem. **271:** 25019–25026.

Umbach, A.L., and Siedow, J.N. (1997). Changes in the redox state of the alternative oxidase regulatory sulfhydryl/disulfide system during mitochondrial isolation: Implications for inferences of activity *in vivo.* Plant Sci. **123:** 19–28.

Umbach, A.L., Wiskich, J.T., and Siedow, J.N. (1994). Regulation of alternative oxidase kinetics by pyruvate and intermolecular disulfide bond redox status in soybean mitochondria. FEBS Lett. **348:** 181–184.

Vanlerberghe, G.C., Day, D.A., Wiskich, J.T., Vanlerberghe, E.A., and McIntosh, L. (1995). Alternative oxidase activity in tobacco leaf mitochondria. Dependence on tricarboxylic acid cycle-mediated redox regulation and pyruvate activation. Plant Physiol. **109:** 353–361.

Vanlerberghe, G.C., and McIntosh, L. (1992). Lower growth temperature increases alternative pathway capacity and alternative oxidase protein in tobacco. Plant Physiol. **100:** 115–119.

Vanlerberghe, G.C., and McIntosh, L. (1996). Signals regulating the expression of the nuclear gene encoding alternative oxidase of plant mitochondria. Plant Physiol. **111:** 589–595.

Vanlerberghe, G.C., and McIntosh, L. (1997). Alternative oxidase: From gene to function. Annu. Rev. Plant Physiol. Plant Mol. Biol. **48:** 703–734.

Vanlerberghe, G.C., Vanlerberghe, A.E., and McIntosh, L. (1994). Molecular genetic alteration of plant respiration. Plant Physiol. **106:** 1503–1510.

Vanlerberghe, G.C., Yip, J.Y.H., and Parsons, H.L. (1999). In organello and in vivo evidence of the importance of the regulatory sulfhydryl/disulfide system and pyruvate for alternative oxidase activity in tobacco. Plant Physiol. **121:** 793–803.

Wagner, A.M. (1995). A role for active oxygen species as second messengers in the induction of alternative oxidase gene expression in *Petunia hybrida* cells. FEBS Lett. **368:** 339–342.

Wagner, A.M., and Krab, K. (1995). The alternative respiration pathway in plants: Role and regulation. Physiol. Plant **95:** 318–325.

Wei, Z.M., Laby, R.J., Zumoff, C.H., Bauer, D.W., He, S.Y., Collmer, A., and Beer, S.V. (1992). Harpin, elicitor of the hypersensitive response produced by the plant pathogen *Erwinia amylovora.* Science **257:** 85–88.

Xie, Z., and Chen, Z. (2000). Harpin-induced hypersensitive cell death is associated with altered mitochondrial functions in tobacco cells. Mol. Plant Microbe Interact. **13:** 183–190.

Yip, J.Y.H., and Vanlerberghe, G.C. (2001). Mitochondrial alternative oxidase acts to dampen the generation of active oxygen species during a period of rapid respiration induced to support a high rate of nutrient uptake. Physiol. Plant **112:** 327–333.